KSTAR Equilibrium Operating Space and Projected Stabilization at High Normalized Beta

Y.S. Park 1), S.A. Sabbagh 1), J.W. Berkery 1), J.M. Bialek 1), Y.M. Jeon 2), S.H. Hahn 2), N. Eidietis 3), T.E. Evans 3), H.L. Yang 2), J. Chung 2), M. Kwon 2), J.Y. Kim 2), S.G. Lee 2), H.K. Park 4), H. Reimerdes 1), J. Leuer 3), M. Walker 3), S.W. Yoon 2), K.-I. You 2)

1) Department of Applied Physics and Applied Mathematics, Columbia University, New York, NY, USA
2) National Fusion Research Institute, Daejeon, Korea
3) General Atomics, San Diego, CA, USA
4) Pohang University of Science and Technology, Korea

e-mail contact of main author: ypark@pppl.gov

Abstract. Along with an expanded evaluation of the equilibrium operating space of the Korea Superconducting Tokamak Advanced Research, KSTAR, experimental equilibria of the most recent plasma discharges were reconstructed using the EFIT code. In near-circular plasmas created in 2009, equilibria have reached stored energy 54 kJ, plasma internal inductance 1.0 with a maximum plasma current 0.34 MA, and transiently reached normalized beta 0.9. Projecting active and passive stabilization of global MHD instabilities for operation above the ideal no-wall beta limit using the designed control hardware is also considered. Kinetic modification of the ideal MHD n = 1 stability criterion was computed by the MISK code on KSTAR theoretical equilibria with plasma current 2 MA, internal inductance 0.7, and normalized beta 4.0 with simple density, temperature and rotation profiles. The steep edge pressure gradient of this equilibrium results in the need for significant plasma toroidal rotation to allow thermal particle kinetic resonances to stabilize the RWM. The impact of various materials and electrical connections of the passive stabilizing plate on RWM growth rates was analyzed, and copper plates reduce the RWM passive growth rate by a factor of 15 compared to SS at normalized beta 4.4. Computations of active RWM control using the VALEN code show that the n = 1 mode can be stabilized at normalized beta near the ideal wall limit via control fields produced by the midplane IVCC with as low as 1.58 kW control power. The ELM mitigation potential of the IVCC, examined by evaluating the island overlap created by resonant magnetic perturbations (RMP), is analyzed using the TRIP3D code. Using a combination of all IVCCs with dominant n = 2 field and upper/lower coils in an even parity configuration, a Chirikov parameter near unity at normalized poloidal flux 0.83, an empirically-determined condition for ELM mitigation in DIII-D, was generated in theoretical high beta equilibria. Chirikov profile optimization is addressed in terms of coil parity, normalized beta and safety factor profile.

1. Introduction

The Korea Superconducting Tokamak Advanced Research, KSTAR, [1] is designed to produce steady-state high beta plasmas to establish the scientific and technological basis of an attractive fusion reactor, and will provide research supporting advanced scenario operation of ITER. A highly shaped plasma having a double null configuration will be operated for a pulse length up to 300 s. The KSTAR design includes a mode control system comprised of passive stabilizing plates and a uniquely designed in-vessel control coil (IVCC) capable of several roles including error field correction and resistive wall mode control. Projecting active and passive stabilization of global MHD instabilities for operation above the ideal no-wall beta limit using the designed control hardware is therefore an important study. Determining the potential for ELM mitigation by resonant magnetic perturbations generated by favorable configurations of the IVCC is another key study. This research is addressed in the present work, along with an expanded evaluation of the equilibrium operating space, and reconstruction of the most recent experimental plasma discharges.

2. Equilibrium Reconstruction

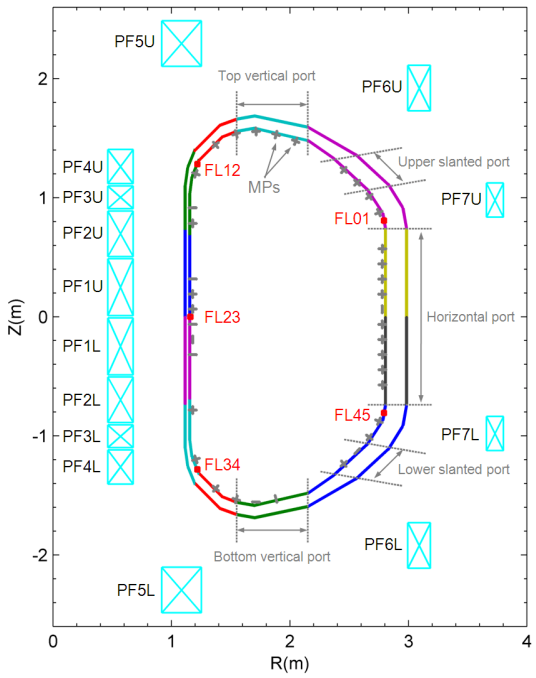

FIG. 1: KSTAR configuration used in equilibrium reconstruction. Major port penetrations are indicated by dashed lines.

KSTAR has a major radius, R_0 = 1.8 m, minor radius, a = 0.5 m, and maximum design toroidal field, B_t = 3.5 T. In 2009, ohmically heated plasmas were created reaching a maximum plasma current, I_p = 0.34 MA, B_t = 2.2 T and maximum pulse lengths up to 4 s. This initial device operation produced near-circular plasmas (κ up to 1.08). Experimental equilibria were reconstructed over the full discharge evolution using the EFIT code. Data from 14 PF coil currents, 67 integrated magnetic pickup loops, 5 flux loop voltage monitors and a Rogowski coil measuring toroidal plasma current were used as constraints. Device vessel currents were included by fitting estimated values based on five loop voltage measurements and effective vessel resistivities from a VALEN code start-up calculation. In the 3D VALEN calculation, non-axisymmetric currents flowing around all port penetrations on the double-walled vacuum vessel are included. Relatively small penetrations by the vertical and slanted ports results in 10% reduction of total vessel current compared to the case considering only large horizontal port penetrations. Figure 1 illustrates the 2D structure of conductors, PF coils, magnetic pickup loops and flux loops used in the EFIT calculation. To increase convergence reliability, the vessel current is represented by 12 independent current carrying groups indicated by regions of different colors in the figure. This allows reasonable representation of the poloidal distribution of the toroidal current on the wall and also the increased resistance by the major port penetrations. The accuracy of the vessel current estimation model is confirmed by comparing the reconstructed vessel current with measurement from vessel current monitor (VCM03) for many vacuum discharges. A simple plasma basis function model constraining p' and ff' to both be zero at the plasma edge is used for reliable reconstruction of near circular plasmas. For many plasma discharges, details of the plasma dynamics and plasma parameter evolutions are investigated. The reconstruction showed good agreement with measured currents and magnetic probe signals for many plasma discharges spanning different operational parameter range. Plasma movement between limiters in experiments is well tracked by reconstructions and compares well to visible plasma images from a fast framing camera. In most of the reconstructed equilibria, the plasma is downshifted from the midplane which may be due to additional current flowing in the bottom of cryostat structure.

In KSTAR, magnetic nonlinearities caused by paramagnetic Incoloy materials used in some of the PF coils causes certain inconsistencies between measured and reconstructed signals. These inconsistencies are mitigated by simple allowance of higher errors for PF coils. Specifically, among the 5 PF coils containing Incoloy (PF1~5), PF1-2 are found to carry most of the compensating current to better match magnetic measurements. In the reconstructions, relatively large errors are set in these two PF coils only, with reduced errors in the other PFs. The discrepancies in signals are mostly balanced by this change, and individual vessel group current and total vessel current show better agreement. Figure 2 shows the reconstructed PF

1-2 currents, total vessel current and MP4P18R magnetic probe signal with different errors set on PF coils. The MP4P18R is an inboard radial magnetic field probe proximate to the two PF coils. Increased PF error clearly improves the total vessel current, and the initial offset of the probe signal is noticeably mitigated by the compensation by the PFs.

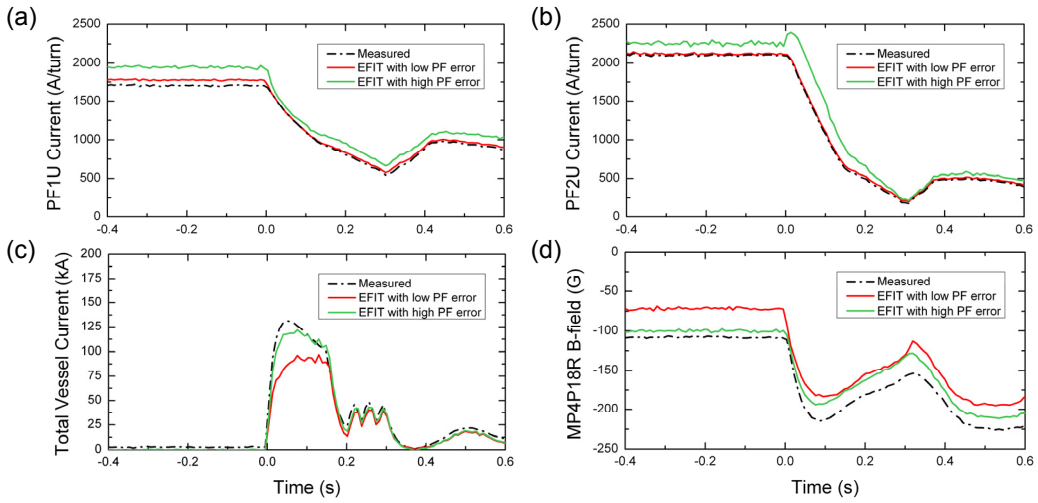

FIG. 2: EFIT vacuum field reconstruction for shot 1845 by using different PF errors. In the low PF error case, relative error σ_{rel} = 0.5% is given to all PFs and is increased to 8%, 10% for PF1-2, respectively, in the high error case. (a) Measured and reconstructed current in PF1U coil and (b) PF2U. (c) Total vessel current compared to measured signal from VCM03. (d) MP4P18R signal.

In plasmas near maximum stored energy, equilibria have reached plasma current, I_p = 335 kA, stored energy 54 kJ, and normalized beta, β_N = 0.68, with plasma internal inductance, l_i = 1.0. An overlay of a reconstruction showing equilibrium flux surfaces and visible light emission from the plasma at the time of maximum plasma stored energy is shown in Fig. 3 with the evolution of the reconstructed stored energy, β_N, and plasma position parameters.

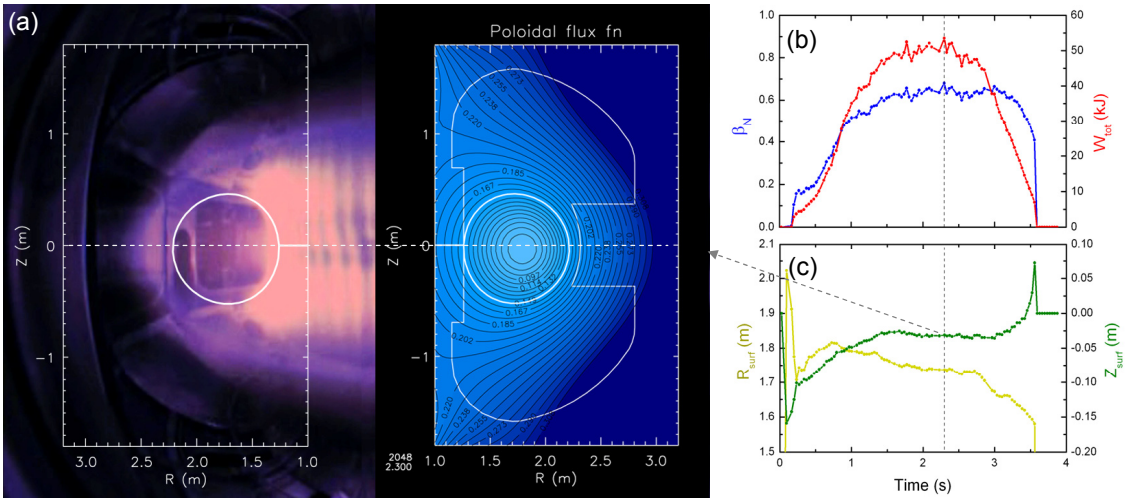

FIG. 3: (a) Fast framing camera image and reconstructed equilibrium flux surfaces at t = 2.3 sec for shot 2048. Only the LCFS is overlaid in the left side of the image. (b) Evolution of reconstructed normalized beta and total plasma stored energy and (c) plasma radial and vertical locations.

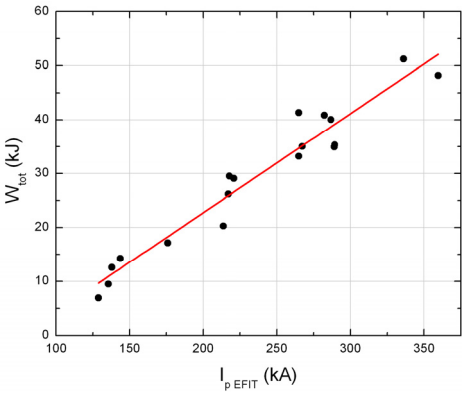

FIG. 4: Variation of W_{tot} versus reconstructed plasma current in 18 ohmic KSTAR equilibria.

To confirm uncertainty in the reconstructed plasma stored energy, Fig. 4 illustrates the variation of W_{tot} as a function of the reconstructed plasma current in 18 equilibria distributed over wide range of I_p. Both parameters are in good linear correlation in these ohmic discharges and the standard error in W_{tot} estimated from the linear fit shown in the figure is about ± 3 kJ.

Reconstructions continue to be developed to improve the vessel current model and the reliability of convergence at all times during the discharge. In the 2010 experimental campaign, reconstruction of highly shaped equilibria will be examined with an updated conducting structure model including newly installed internal hardware such as passive plates and divertors.

3. RWM Stability Modification by Kinetic Effects

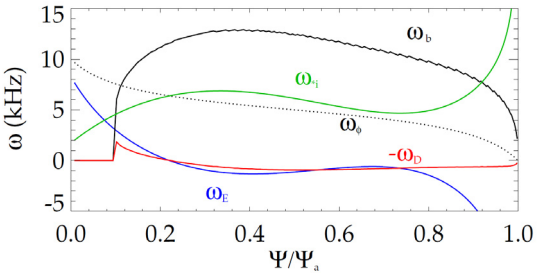

FIG. 5: Profiles of ω_φ, ω_{*i}, the resulting ω_E, and ω_b and $-\omega_D$ with zero pitch angle and ε/T = 2 and 3/2, respectively (see Ref. [5]).

At maximum design I_p = 2 MA, ideal MHD stability calculations of theoretical equilibria show n = 1 no-wall and with-wall β_N limits ranging from 2.5-3.5 and 4.5-5.0 respectively with l_i between 0.6-0.9 for pressure profiles taken from DIII-D H-mode plasmas [2]. Kinetic modification of the ideal MHD n = 1 stability criterion, computed by the MISK code [3], has been used successfully to analyze resistive wall mode (RWM) stability in NSTX [4-6]. Similar analysis was performed on KSTAR theoretical equilibria with I_p = 2 MA, l_i = 0.7, and β_N = 4.0 with density ($n_e = n_i$) and temperature ($T_e = T_i$) profiles similar to DIII-D (density gradient steeper than temperature), and a plasma rotation profile similar to NSTX (which has all co-directed beams). Shown in Fig. 5 are plasma rotation frequency profile, ω_φ, the ion diamagnetic frequency ω_{*i} resulting from the density and temperature profiles, the resulting *ExB* frequency profile, and the precession drift and bounce frequency profiles. The steep edge pressure gradient of this equilibrium causes a large ion diamagnetic frequency and a large negative *ExB* frequency near the edge.

Figure 6 is a stability diagram similar to those in Refs. [4-6] which shows MISK calculated $Im(\delta W_K)$ vs. $Re(\delta W_K)$ with a backdrop of contours of constant $\gamma\tau_w$ for varying magnitude of rotation profiles. The results indicate that for the profiles chosen, resonance

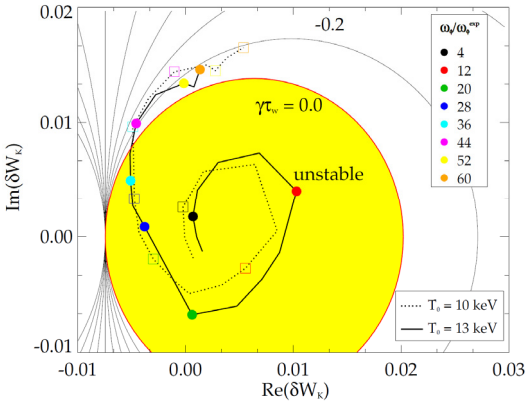

FIG. 6: Stability diagram for theoretical β_N = 4.0 KSTAR equilibrium with varied rotation profiles of the shape shown in Fig. 5, with $\omega_{\varphi 0}$ from 0-60 kHz.

between the mode and the trapped thermal ion precession drift is insufficient to stabilize the RWM. When this resonance occurs over much of the plasma radius, at $\omega_{\varphi 0}$ = 10 kHz (Fig. 5), it contributes to δW_K, as shown in Fig. 6, but without resonance in the outer surfaces where the RWM eigenfunction is large, the mode remains unstable. This leads to a relatively large rotation $\omega_{\varphi 0} \sim$ 42 kHz required for stability with T_0 = 13 keV, n_0 = 1.3e20 m^{-3}, and $\omega_{\varphi 0} \sim$ 34 kHz with T_0 = 10 keV, n_0 = 1.7e20 m^{-3}.

A test of the effect of energetic particles (EPs) in stabilizing the RWM in KSTAR was performed by assuming that 20% of the total pressure is from energetic ions. The EP pressure profile shape was taken as the same as the total pressure, a simple isotropic slowing-down distribution function was assumed [6], and the thermal ion and electron densities were reduced by 20% so that the total pressure would remain consistent with the equilibrium. Interestingly, EPs were found to have very little stabilizing effect in this case, which is in contrast to results from NSTX [6] and DIII-D [7]. Further investigation is needed to determine the cause, as well as determine the sensitivity of the results to the profiles chosen.

4. Passive & Active Stabilization of RWM

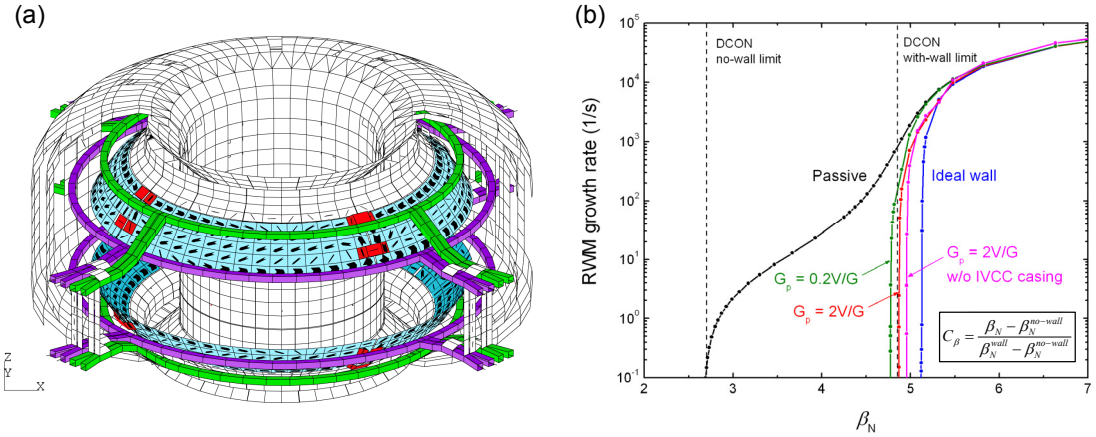

FIG. 7: (a) KSTAR conducting structure and IVCC with surrounding conductive casing in the VALEN model. (b) RWM growth rate vs. β_N with different controller gains. The finalized stabilizing plate design and 8 toroidal midplane B_p sensors for n =1 mode identification are used in the calculation.

Design of the KSTAR stabilizing plates was finalized in 2009 after considering the impact of various materials and electrical connections on RWM passive growth rates. The final design utilizes copper plates, each having four high resistance toroidal breaks. The current bridges were eliminated as they do not greatly impact the RWM growth rate and increase the potential for error fields. Copper plates reduce the RWM growth rate by a factor of 15 compared to SS at β_N = 4.4 (92% of the n = 1 with-wall limit).

Computations of active RWM control using the VALEN code show that the n = 1 mode can be stabilized at β_N near the ideal wall limit via control fields produced by the middle-FEC coil displayed in purple in Fig. 7a. The middle-FEC coil comprises four independently operated toroidal sector coils and each sector has 2-turn copper coil with a surrounding 3 mm thick SS coil casing. The circuit parameters for each middle-FEC coil are L = 44 μH, R = 3.66 mΩ with L/R = 12 msec in VALEN calculations. A single n = 1 unstable eigenfunction from l_i = 0.7 and β_N = 5.0 KSTAR equilibrium with H-mode pressure profile is used in the calculation [2]. The growth rate calculation indicates that the plasma can be stabilized up to the with-wall limit predicted by DCON, which corresponds to C_β = 99% with

controller gain, G_p = 2 V/G; C_β = 95% can be reached with this gain reduced by an order of magnitude. The presence of conductive coil casing shows a small degradation of control performance, which results in the reduction of C_β by about 5% using the same controller gain.

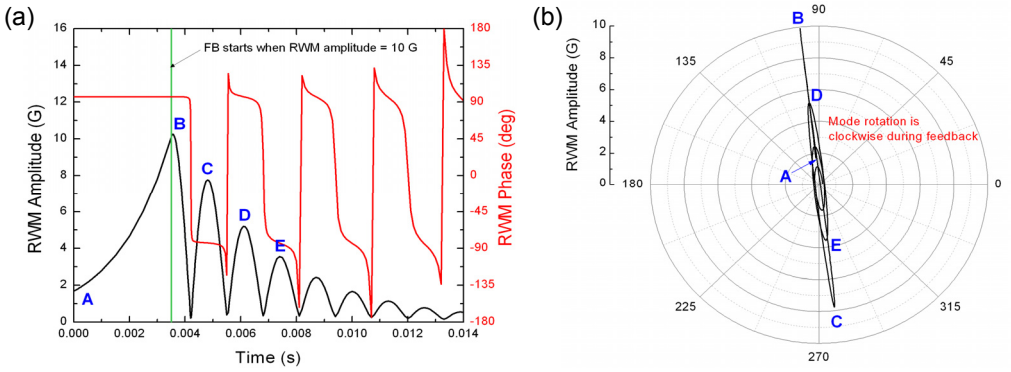

FIG. 8: (a) RWM amplitude and phase during feedback stabilization with stable feedback phase. (b) Polar plot of RWM behavior during feedback.

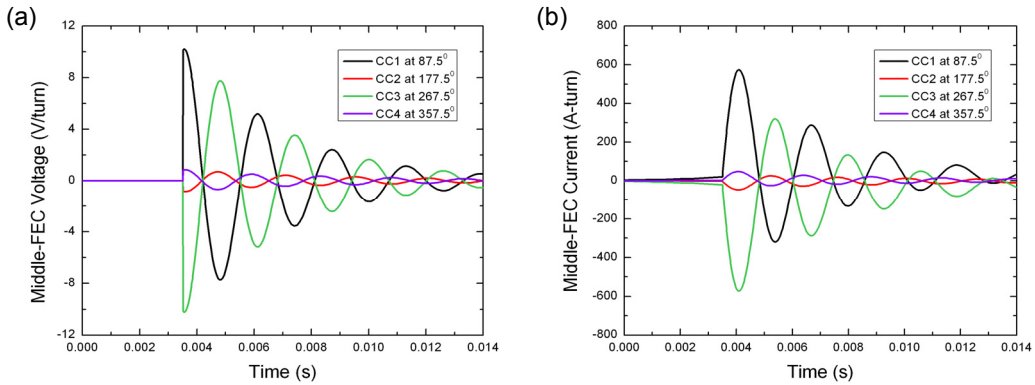

FIG. 9: (a) Control coil voltages vs. time in the feedback stabilization in Fig. 8. (b) Control coil currents.

Power requirements for RWM stabilization are calculated from time domain feedback control simulation for a highly unstable mode at β_N = 4.8 close to the with-wall limit, with a feedback gain 2 V/G. Mode rotation with respect to the plasma, which usually has a stabilizing effect, is excluded and an ideal control system without noise or time delay is assumed. Feedback is started when the mode amplitude becomes 10 G and the mode is fully suppressed by the applied feedback gain and phase and exhibits clockwise mode rotation as shown in Fig. 8. RMS values of the required coil currents, voltages and power is summarized in table 1. For this simulation, less than 575 A-turn and 10.2 V/turn, peak, are required for each coil and the total RMS power is estimated as 1.58 kW for the entire middle-FEC coil set. Further calculations with decreased L/R time for faster feedback responses are being made to determine the effect on power requirements.

	CC1 (87.5°)	CC2 (177.5°)	CC3 (267.5°)	CC4 (357.5°)
P_{RMS} (W)	785.4	5.8	785.4	5.8
I_{RMS} (A)	181.5	16.5	181.5	16.5
V_{RMS} (V)	2.72	0.27	2.72	0.27

Table 1: Control power requirement for RWM stabilization using middle-FEC coils.

5. Potential for ELM Mitigation by RMP

The edge localized mode (ELM) mitigation potential of the IVCC, examined by evaluating the island overlap created by resonant magnetic perturbations (RMP), is analyzed using the TRIP3D code. Using a combination of all IVCCs (top, bottom and middle FEC coils) generating dominant n = 2 resonant field spectrum, the appropriate RMP configuration is investigated in terms of the RMP spectrum pitch alignment with safety factor in the plasma edge and critical location where the Chirikov parameter, which denotes degree of island overlap, becomes unity. A theoretical equilibrium having q_{95} = 3.6 and β_N = 2.5 with H-mode pressure profile is used in the analysis.

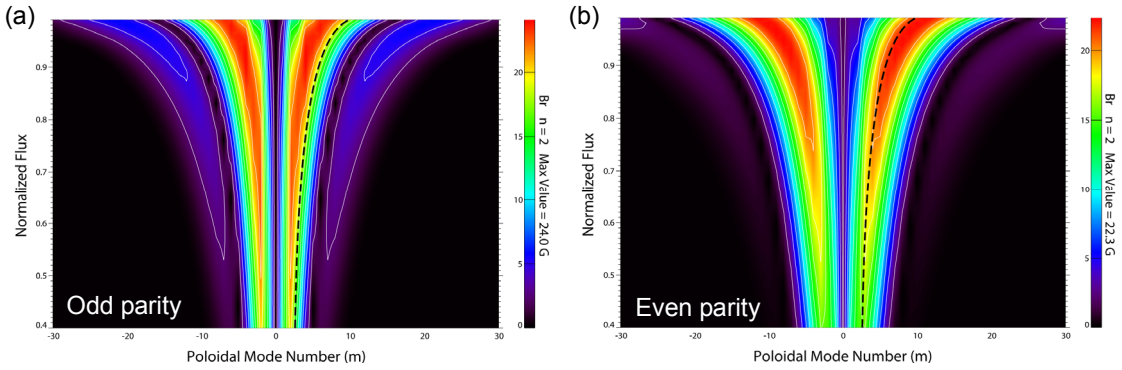

FIG. 10: (a) Contours of poloidal mode spectrum (-30 < m < 30) of n = 2 perturbation from IVCC in odd parity configuration and (b) even parity configuration for a theoretical equilibrium having β_N = 2.5, q_{95} = 3.6. The equilibrium q-profile is shown with a black dashed line.

Figure 10 shows pitch resonances of two different coil current parities using the 24 kA of absolute coil current, odd parity with (top, middle, bottom FECs) = (+12, 0, -12) kA and even parity with (+8, -8, +8) kA. ELM suppression is expected when the resonant field spectrum is well aligned with the q-profile in the edge region. The resonant field distribution is quite different according to the parity condition. Odd parity has relatively lower m-spectrum caused by utilizing only 2 coils poloidally separated and it perturbs more into the core region. A ridge of the resonant field distribution is marginally aligned with the q-profile on the region of right-handed higher m-harmonics. Therefore, this perturbation is not efficiently coupled to the equilibrium rational surfaces. With even parity, a ridge is localized around the edge of the plasma with higher m-numbers leading to better pitch alignment with the q-profile and less resonance with core harmonics. Global pitch alignment in odd parity is possible for lower q-profile but then a larger overlap between the two large m/n = 3/2 and 4/2 islands can be detrimental. The other advantageous aspect of even parity is that the amount of middle-FEC current can change the applied m-spectrum so it is more amenable to different q-profiles. For instance, even parity can also make good pitch alignment with an equilibrium having lower l_i = 0.7 with elevated q-profile (q_{95} = 4.5) excluding a large 3/2 island, whereas a ridge of odd parity lying in the lower-m region is

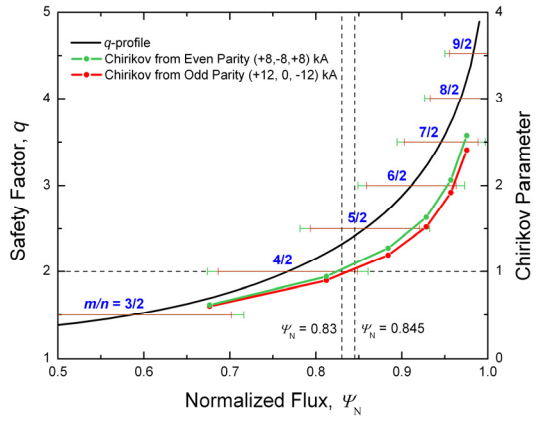

FIG. 11: Vacuum Chirikov profiles and n = 2 resonant harmonic island widths from the even and odd parity cases shown in Fig. 10.

not favorable to make good pitch alignment with higher q [8].

Calculations of the locations and widths of the islands resulting from RMP in Fig. 11 indicate that the islands are well overlapped to form stochastic field lines in the edge. Island widths are larger in even parity than those in odd parity due to better pitch alignment with higher resonant normal field. Islands from other n-harmonics are negligibly small and excluded in the Chirikov calculation. In even parity, the islands start to significantly overlap and the Chirikov parameter exceeds unity from $\Psi_N = 0.83$ which is an empirically determined condition for ELM mitigation in DIII-D [9]. The odd parity case creates edge stochastization in the higher Ψ_N region. In this moderate q_{95} equilibrium, large growth of 3/2 and 4/2 islands is caused by RMP which poses a potential loss of overall confinement via triggering of neoclassical tearing modes. Further investigation is needed for utilizing RMP using higher n-spectra for a possible IVCC upgrade.

6. Conclusions

Experimental equilibria of recent KSTAR discharges were reconstructed using the EFIT code, including theoretically estimated vessel current and reasonable compensation of the Incoloy effect. The reconstruction showed good agreement with measured signals and important plasma internal parameters were obtained as a useful evaluation for the discharges. Based on the previous effort dedicated to theoretical equilibrium and stability of KSTAR plasmas, research regarding global MHD stabilization has been performed. Kinetic modification of ideal $n = 1$ stability, which has been successfully used in NSTX, indicates that relatively large rotation would be required to obtain RWM stability. A design of the passive stabilizing plates was finalized to have maximum RWM passive stabilization, and a time dependent control simulation showed that the mode can be actively stabilized by using the middle-FEC coil with 1.58 kW RMS control power. The ELM mitigation potential using RMP from IVCC has been studied by estimating island overlap using different coil parities. Higher m-spectrum from up-down even parity configuration with aid from the middle-FEC coil would be better to obtain favorable pitch alignment not only with a conventional q-profile but also with elevated q-profiles suitable for advanced tokamak operation. Work continues to develop useful guidance for stabilization in future KSTAR high beta equilibria. This research was supported by the U.S. Department of Energy under contract DE-FG02-99ER54524.

References

[1] LEE, G.S., KIM, J., HWANG, S.M., et al., Nucl. Fusion **40** (2000) 575.
[2] KATSURO-HOPKINS, O., SABBAGH, S.A., BIALEK, J.M., et al., Nucl. Fusion **50** (2010) 025019.
[3] HU, B., BETTI, R., and MANICKAM, J., Phys. Plasmas **12** (2005) 057301.
[4] SABBAGH, S.A., BERKERY, J.W., BELL, R.E., et al., Nucl. Fusion **50** (2010) 025020.
[5] BERKERY, J.W., SABBAGH, S.A., BETTI, R., et al., Phys. Rev. Lett. **104** (2010) 035003.
[6] BERKERY, J.W., SABBAGH, S.A., REIMERDES, H., et al. Phys. Plasmas **17** (2010) 082504.
[7] SABBAGH, S.A., et al. "Resistive Wall Mode Stabilization and Plasma Rotation Damping Considerations for Maintaining High Beta Plasma Discharges in NSTX," this conference.
[8] KIM, D., HAN, H., KIM, K.M., et al., Plasma Phys. Control. Fusion **52** (2010) 095009.
[9] FENSTERMACHER, M.E., EVANS, T.E., OSBORNE, T.H., et al., Phys. Plasmas **15** (2008) 056122.